Impact of Voltage Source and Initial Conditions on the Initiation of Ferroresonance

KRUNO MILIČEVIĆ, IVAN RUTNIK - *Faculty of Electrical Engineering, Osijek*
IGOR LUKAČEVIĆ - *HEP-Transmission system operator Ltd, Osijek*
CROATIA
http://www.etfos.hr; http://www.hep.hr

Abstract: The impact of voltage source and initial conditions on the initiation of ferroresonance is investigated. The investigation is carried out by simulating the behaviour of the mathematical model of ferroresonant circuit realized in the laboratory. The initiation of ferroresonance is investigated by varying the values of phase shift and amplitude of voltage source in order to incite the ferroresonance. Thereby, the initial conditions are varied within a practically possible range of initial values of transformer voltage and transformer flux linkage.

Key-Words: Ferroresonance, Iron-cored reactor, Bifurcation diagram, Chaos, Nonlinear circuits

1 Introduction

The simple electrical circuit in which ferroresonant oscillation can occur is a circuit which comprises a linear capacitor in series with a nonlinear coil, driven by a sine-wave voltage source, Fig. 1. The nonlinearity of the coil comes from the nonlinear magnetization characteristic of the iron core.
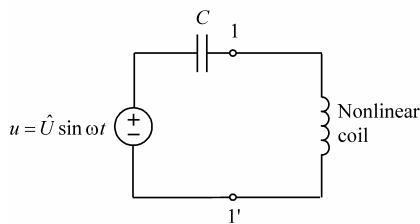
Fig. 1. Ferroresonant circuit

The usual electrical model of the nonlinear coil is a nonlinear reactor described by $i_L(\varphi)$ characteristic in parallel with a nonlinear resistor described by $i_R(u_L)$ characteristic, Fig. 2.
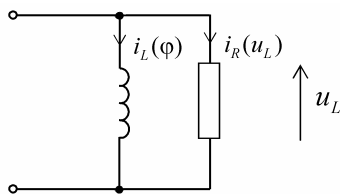
Fig. 2. Model of nonlinear coil

The nonlinear coil is realized either as a winding of the unloaded iron-cored transformer or as a winding of the iron-cored reactor without air gap. The analyzed circuit is a laboratory model, but in praxis it is a simplest physical model of a large electrical power system for the ferroresonance case studies. An example of ferroresonance in three phase transmission system is shown on Fig. 3.
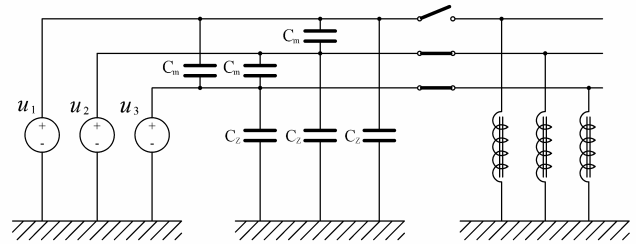
Fig. 3. Ferroresonance in three phase system

The nonlinear inductances represent iron core coils of unloaded three phase power transformer and the capacitance (C_m, C_Z) represents capacitance of long transmission line (or HV underground cable). In this case, the ferroresonance occurs because of the malfunction of one pole of HV circuit breaker. The Fig. 1 shows the equivalent circuit where

$$u = (u_2 + u_3)\frac{C_m}{2C_m + C_Z}$$
$$C = 2C_m + C_Z \qquad (1)$$

More practical examples are described in the literature [1].

Ferroresonant circuit is a nonlinear dynamical system and as such several steady-state responses of the circuit can be obtained: monoharmonic, odd

Corresponding author. K. Milicevic is with the Faculty of Electrical Engineering, Osijek, Croatia (e-mail: kruno.milicevic@etfos.hr). Tel: 00385912246021; Fax: 0038531224708.

higher harmonic, even and odd higher harmonic, subharmonic and chaotic steady-state response, [1-4].

Sudden change of steady-state types caused by a small change made to the parameter values is named as a bifurcation [5]. In a ferroresonant circuit, bifurcations that cause a change from monoharmonic to any polyharmonic steady-state with significantly higher state-variable values are usually named as a ferroresonance. Three basic types of ferroresonance can be identified [2, 3]: the fundamental frequency ferroresonance [6], subharmonic ferroresonance, where the period of oscillation is an integral multiple of the period of the supply system, and chaotic ferroresonance, in which the oscillations appear to be random.

Each type of ferroresonance can destroy parts of electrical power network [7]-[9]. Thus, it is too expensive to investigate the ferroresonance on an electrical power network by varying the parameter values of the network.

Therefore, the ferroresonant circuit realized in the laboratory is used as a physical model of ferroresonant part of electrical power network, in order to investigate impact of source voltage on the initiation of steady-state types. The circuit is named here as the laboratory ferroresonant circuit.

Thereby, steady-state types of the laboratory ferroresonant circuit are obtained for a fixed set of parameters and by varying the voltage source amplitude $\hat{U}$ only.

From engineering point of view it is important to predict the bifurcation points, i.e. the values of voltage source amplitude at which the change of steady-state responses takes place. Furthermore, the results of investigation of the ferroresonant circuit could be applied to other electrical nonlinear systems [10-12], as well as to the non-electrical nonlinear systems [13].

2 Laboratory ferroresonant circuit

In order to investigate impact of parameter values in a controlled manner, without the danger of destruction of components, the laboratory ferroresonant circuit, being composed of the linear capacitor C=20 μF and the nonlinear coil, is realized in the laboratory.

The primary winding of the toroidal iron-cored two-winding transformer was used as a nonlinear coil. The transformer was designed for the nominal apparent power of 200 VA and for the nominal

primary voltage of 30 V. The core was strip--wounded, made of Ni-Fe alloy (Trafoperm N3). The autotransformer of 10 kVA nominal apparent power was used as a variable voltage source in all experiments.

All the variables and parameters of the ferroresonant circuit are expressed in relation to reference quantities; that is, in a per-unit system:

$$\overline{\varphi} = \varphi \frac{\omega}{U_{ref}}; \overline{u}_C = \frac{u_C}{U_{ref}}; \overline{\omega} = \frac{\omega}{\omega_{ref}}; \overline{i}_L = \frac{i_L}{I_{ref}}; \hat{\overline{U}} = \frac{\hat{U}}{U_{ref}}$$

The referent time value is chosen to be $\omega_{ref}=2\pi f$, f=50Hz. The reference voltage and current are obtained at the intersection point of the RMS voltage versus RMS current characteristics of the capacitor and the nonlinear coil, Fig. 4. They are: U_{ref}=31.2 V, I_{ref}=0.19 A.
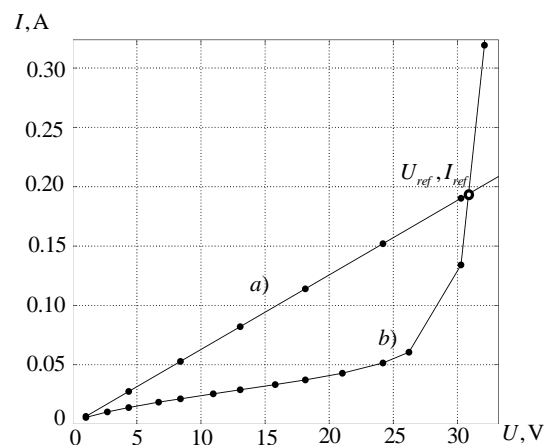
Fig. 4. Measured RMS voltage/current characteristics of: a) capacitor and b) nonlinear coil.

Bifurcations and steady-state types shown on Table 1 are obtained by varying the voltage source amplitude in a range $0 < \hat{\overline{U}} \le 3$, i.e. by increasing the voltage source amplitude from value $\hat{\overline{U}} \approx 0.05$ to the value $\hat{\overline{U}} = 3$, and by decreasing the voltage source amplitude from value $\hat{\overline{U}} = 3$ to the value $\hat{\overline{U}} \approx 0.05$. The voltage source amplitude is varied in steps of $\Delta\hat{\overline{U}} \approx 0.05$.

Fig. 5 shows results of measurements presented as a 1-parameter bifurcation diagram. The 1-parameter bifurcation diagram was obtained by periodic stroboscoping of coil flux $\overline{\varphi}(t)$, [14].

Table 1 Steady-states and *bifurcations* of the ferroresonant circuit obtained by measurements.

Increasing $\hat{\bar{U}}$	Decreasing $\hat{\bar{U}}$	Steady-states and bifurcations
$0 \leq \hat{\bar{U}} < 1$	$0 \leq \hat{\bar{U}} < 0.7$	Monoharmonic steady-state
$\hat{\bar{U}} = 1$	-	*Forward ferroresonant jump*
-	$\hat{\bar{U}} = 0.7$	*Reverse ferroresonant jump*
$1 < \hat{\bar{U}} < 1.4$	$0,7 < \hat{\bar{U}} < 1.4$	Odd higher harmonic steady--state
$\hat{\bar{U}} = 1.4$		*Pitchfork bifurcation*
$1.4 < \hat{\bar{U}} < 2.4$		Even and odd higher harmonic steady-state
$\hat{\bar{U}} = 2.4$		*First period--doubling bifurcation*
$2.4 < \hat{\bar{U}} < 2.7$		Period-two steady--state
$2.7 \leq \hat{\bar{U}} \leq 3$		Chaotic steady--state

The voltage source amplitude $\hat{\bar{U}}$ was increased/decreased continuously, i.e. the amplitude was increased/decreased at the value $\hat{\bar{U}} \pm \Delta \hat{\bar{U}}$ after the steady-state, obtained for the value $\hat{\bar{U}}$, has been established and identified.
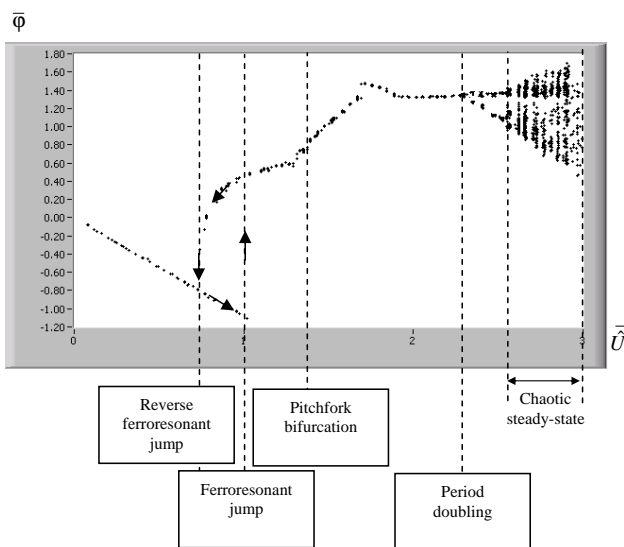
Fig. 5. The 1-parameter bifurcation diagram obtained by measurements.

Thereby, it was practically impossible to vary the initial values of coil voltage $\bar{u}_L(0)$ and flux $\bar{\varphi}(0)$ optionally and to investigate their impact on the initiation of steady-state types experimentally.

Thus, the impact of initial conditions - $\bar{u}_L(0)$ and $\bar{\varphi}(0)$ - on the initiation of steady-state types is investigated by a computer simulation using the mathematical model of the laboratory ferroresonant circuit.

3 Mathematical model of the laboratory ferroresonant circuit

The time domain behaviour of the basic ferroresonant circuit of Fig. 2 can be described by the following differential equations:

$$\frac{d\varphi}{dt} = u_L = \hat{U}\sin(\omega t + \alpha) - u_C$$
$$\frac{du_C}{dt} = \frac{1}{C}\left[\frac{u_C}{R} + i_L(\varphi)\right] \tag{2}$$

Per-unit parameters of the model are obtained using reference values ($U_{ref}=31.2$ V, $I_{ref}=0.19$ A):

$$\bar{\omega} = 1 \; ; \; \bar{C} = 1 \; ; \; \bar{R} = \frac{\bar{u}_L}{\bar{i}_R} = 2$$

$$\bar{i}_L(\bar{\varphi}) = f(\bar{\varphi})\text{sign}(\bar{\varphi})$$
$$f(\bar{\varphi}) = \sqrt{0.034 \cdot \bar{\varphi}^2 + 5.54 \cdot 10^{-3} \cdot \bar{\varphi}^{20} + 1.05 \cdot 10^{-5} \cdot \bar{\varphi}^{38}} \tag{3}$$

Thereby, the magnetization characteristic $\bar{i}_L(\bar{\varphi})$ and the iron-core losses $\bar{R}$ are derived from measured *P-U* and *U-I* characteristics of the nonlinear coil [15].

Equations (2) in all simulations were solved using the commercially available software package MATLAB/Simulink employing the Dormand-Prince method which is the default solver used by Simulink for models with continuous states [16].

4 Preliminary simulations

The preliminary simulations were carried out at the same way as the measurements. Namely, bifurcations and steady-state types shown on Table 2, as well as the 1-parameter bifurcation diagram shown on Fig.6 [14], are obtained by increasing the voltage source amplitude from value $\hat{\bar{U}} = 0.05$ to the value $\hat{\bar{U}} = 3$, and by decreasing the voltage source amplitude from value $\hat{\bar{U}} = 3$ to the value $\hat{\bar{U}} = 0.05$.

Table 2 Steady-states and *bifurcations* of the ferroresonant circuit obtained by preliminary simulations

Increasing $\hat{\bar{U}}$	Decreasing $\hat{\bar{U}}$	Steady-states and bifurcations
$0 \leq \hat{\bar{U}} < 1.05$	$0 \leq \hat{\bar{U}} < 0.7$	Monoharmonic steady-state
$\hat{\bar{U}} = 1.05$	-	*Forward ferroresonant jump*
-	$\hat{\bar{U}} = 0.7$	*Reverse ferroresonant jump*
$1 < \hat{\bar{U}} < 1.8$	$0,7 < \hat{\bar{U}} < 1.8$	Odd higher harmonic steady--state
$\hat{\bar{U}} = 1.8$		*Pitchfork bifurcation*
$1.8 < \hat{\bar{U}} < 2.45$		Even and odd higher harmonic steady-state
$\hat{\bar{U}} = 2.45$		*First period--doubling bifurcation*
$2.45 < \hat{\bar{U}} < 2.65$		Period-two steady--state
$2.65 \leq \hat{\bar{U}} \leq 3$		Chaotic steady--state

The voltage source amplitude $\hat{\bar{U}}$ was increased/decreased at the value of voltage source amplitude $\hat{\bar{U}} \pm \Delta\hat{\bar{U}}$ ($\Delta\hat{\bar{U}} = 0.05, \alpha = 0$) after the steady-state, obtained for the value $\hat{\bar{U}}$, has been established and identified.
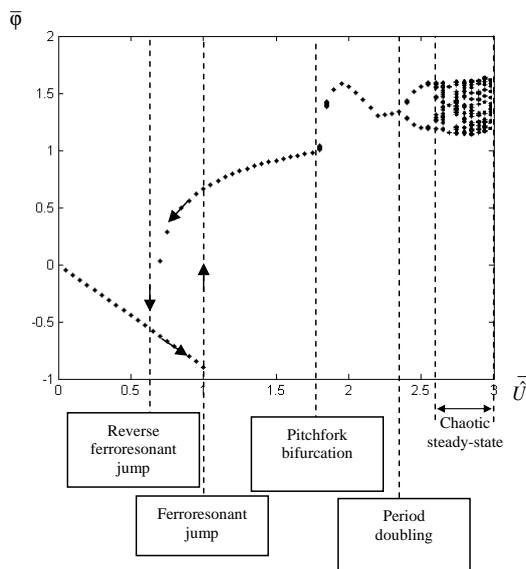
Fig. 6. The 1-parameter bifurcation diagram obtained by simulation.

Initial conditions were set on values $\bar{u}_L(0) = 0$ and $\bar{\varphi}(0) = 0$ at the beginning of simulation only, i.e. at the value of voltage source amplitude $\hat{\bar{U}} = 0.05$.

The most significant disagreement between the results of measurements, Table 1 and Fig. 5, and preliminary simulation, Table 2 and Fig. 6, is the value of voltage source amplitude $\hat{\bar{U}}$ at which the pitchfork bifurcation occurs.

5 Additional simulations

In order to determine the impact of initial conditions on the initiation of steady-state types, additional simulations were carried out by varying the values of voltage source amplitude

$$0 < \hat{\bar{U}} \leq 3$$

phase shift

$$0 \leq \alpha < 2\pi$$

and initial conditions of voltage $\bar{u}_L$ and flux linkage $\bar{\varphi}$.

The initial conditions are varied within the range

$$\bar{u}_L(0)_m = 2\hat{\bar{U}}\left(\frac{m}{50} - 1\right); \quad m = 0,1,...,100 \qquad (4)$$

$$\bar{\varphi}(0)_n = \frac{2\hat{\bar{U}}}{\bar{\omega}}\left(\frac{n}{50} - 1\right); \quad n = 0,1,...,100 \qquad (5)$$

These combinations result into 10201 different sets of initial values and hence as many steady-state solutions for each value of voltage source phase and phase shift.

The dependence of the steady-state solution and consequently the initiation of ferroresonance on initial conditions are depicted in what could be called a 2-parameter bifurcation diagram. For easier visualization the diagrams were constructed using colour coded squares where different colours were employed to represent different steady-state solution.

5.1 Monoharmonic steady-state and odd higher harmonic steady-state

The monoharmonic steady-state and odd higher harmonic steady-state are noticed in preliminary simulations for a range of values of voltage source amplitude $0 < \hat{\bar{U}} < 1.8$. Thus, the impact of initial conditions on the change from monoharmonic steady-state to odd higher harmonic steady-state (ferroresonant jump) and vice versa (reverse

ferroresonant jump) is investigated for this range of values of voltage source amplitude.

For eight different phase shift values, $\alpha = 0, \frac{\pi}{4}, \frac{\pi}{2}, ..., \frac{3\pi}{2}, \frac{7\pi}{4}$, and values of voltage source amplitude $\hat{U} = 0.1, 0.2, ..., 0.6$ obtained steady-state types are monoharmonic steady-states for all initial conditions values defined by (4) and (5).

Fig. 7 shows 2-parameter bifurcation diagrams for voltage source amplitude $\hat{U} = 0.7$, initial conditions defined by (4) and (5), and eight different phase shift values of voltage source.

■ Monoharmonic steady-state
□ Odd higher harmonic steady-state

a)　　　　　　　　　　b)

c)　　　　　　　　　　d)

e)　　　　　　　　　　f)

g)　　　　　　　　　　h)
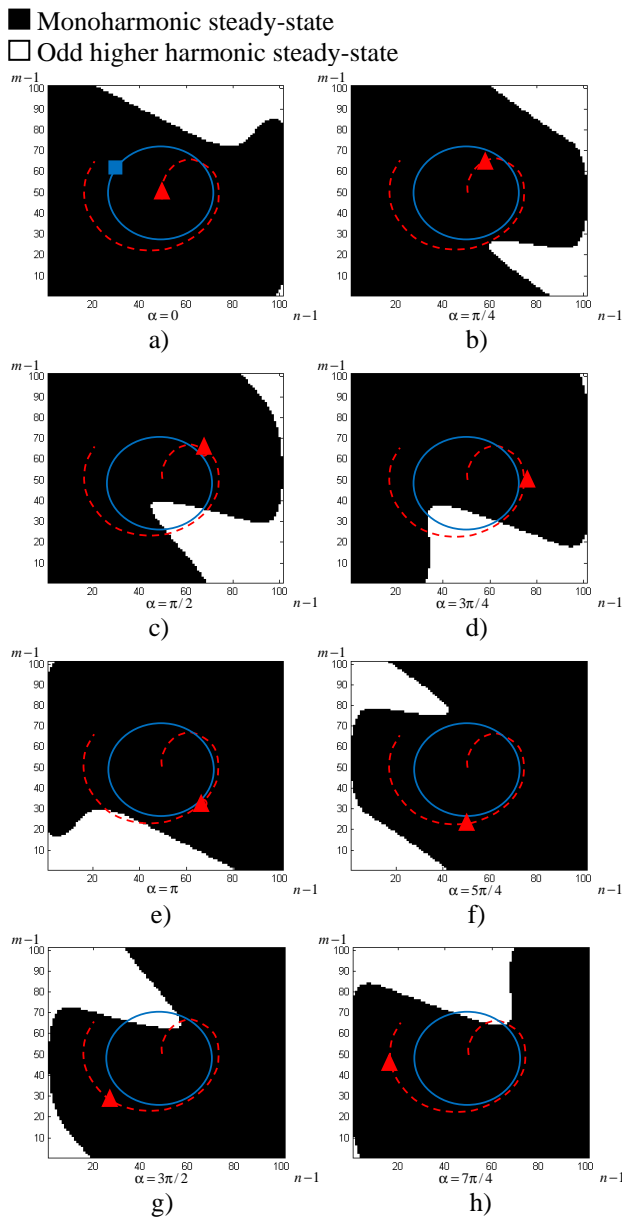
Fig. 7. The 2-parameter bifurcation diagrams for voltage source amplitude $\hat{U} = 0.7$

From these 2-parameter bifurcation diagrams following properties of the diagrams can be concluded:

a) Rotational symmetry

Resultant steady-state solution types shown on Fig. 7 indicate the rotational movement of the area corresponding to the normal sinusoidal steady-state ("black" area) in a clockwise direction.

Consequently, for the steady-state results obtained under phase shift α and for those obtained under $\alpha + \pi$ there is a rotational symmetry in the diagrams.

Namely, the types of steady-state solutions shown on Figs. 7a-7d obtained for initial values $\bar{u}_L(0)_m$ and $\bar{\varphi}(0)_n$ are qualitatively equal to the steady-state solutions shown on Figs. 7e-7h, respectively, obtained for initial values $-\bar{u}_L(0)_m$ and $-\bar{\varphi}(0)_n$, i.e. the Figs. 7a-7d are symmetric to the Fig.7e-7h, respectively, with respect to the angle π.

The rotational symmetry results from the odd symmetry of state-equations of the ferroresonant circuit, (2) and (3).

b) Repetition of steady-state solution types

Steady-state types shown on a bifurcation diagram for a particular value of phase shift will appear also on bifurcation diagrams for any other value of phase shift. For instance, Fig. 8 shows a trajectory of coil voltage and flux obtained by a simulation at the beginning of transient state, i.e. at the interval $0 \le t \le 2\pi$, for voltage source amplitude $\hat{U} = 0.7$, phase shift $\alpha = 0$, and initial conditions $\bar{u}_L(0) = 0$ and $\bar{\varphi}(0) = 0$. Red triangles on Fig. 8 mark the values of coil voltage and flux, $\bar{u}_L(t)$ and $\bar{\varphi}(t)$, in the moments:

$$\Delta t \cdot \frac{\pi}{4} \quad ; \qquad \Delta t = 0, 1, 2, ..., 7 \qquad (6)$$

Instantaneous values of coil voltage and flux in each moment defined by (6):

$$\bar{u}_L\left(\Delta t \cdot \frac{\pi}{4}\right), \bar{\varphi}\left(\Delta t \cdot \frac{\pi}{4}\right)$$

and obtained by simulation for phase shift $\alpha = 0$ can be comprehended as initial conditions
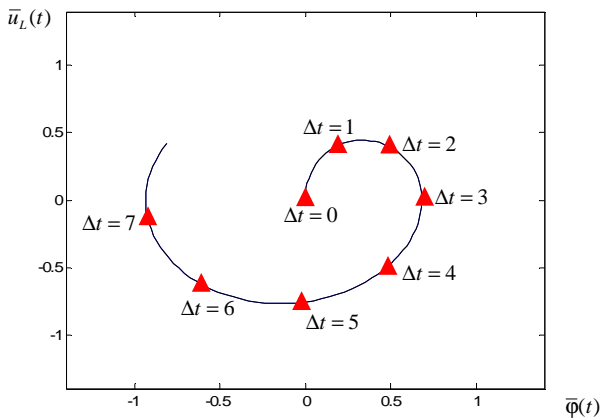
Fig. 8. Trajectory of coil voltage and flux obtained by a simulation at the interval $0 \le t \le 2\pi$ ($\hat{\overline{U}} = 0.7$, $\alpha = 0$, $\overline{u}_L(0) = 0$ and $\overline{\varphi}(0) = 0$).

$\overline{u}_L'(0), \overline{\varphi}'(0)$ in a simulation, the phase shift of which would be $\alpha' = \Delta t \cdot \dfrac{\pi}{4}$. These values are marked on Figs. 7 also. Thereby, it is obvious that, in observed case, for each marked pair of initial conditions the obtained steady-state type would be a monoharmonic steady-state.

Generally, steady state-types obtained for particular values of voltage source amplitude $\hat{\overline{U}}$, phase shift α and initial conditions $\overline{u}_L(0)$ and $\overline{\varphi}(0)$ will be obtained for same value of voltage source amplitude $\hat{\overline{U}}$, and for any values of phase shift α' when the initial conditions are set at values

$$\overline{u}_L'(0) = \overline{u}_L(\alpha' - \alpha)$$
$$\overline{\varphi}'(0) = \overline{\varphi}(\alpha' - \alpha)$$

c) Limitation of initial condition values

Generally, in a simulation the values of initial conditions of the mathematical model, (2) and (3), are optional, (4) and (5). However, in a physical model the values of initial conditions are determined by a previous state of the system. Preliminary simulations were carried out regarding this fact.

Namely, in preliminary simulations, by a continuous varying of the voltage source amplitude the range of possible values of initial conditions, $\overline{u}_L(0)$ and $\overline{\varphi}(0)$, is determined by instantaneous values of coil voltage and flux, $\overline{u}_L(t)$ and $\overline{\varphi}(t)$, that are obtained at the previous value of voltage source amplitude. For instance, in a case of increasing of the voltage source amplitude $\hat{\overline{U}}$ the values of initial conditions, $\overline{u}_L(0)$ and $\overline{\varphi}(0)$, for the value of voltage

source amplitude $\hat{\overline{U}} = 0.7$ can be equal to any pair of instantaneous values, $\overline{u}_L(t)$ and $\overline{\varphi}(t)$, that are obtained at the value of voltage source amplitude $\hat{\overline{U}} - \Delta\hat{\overline{U}} = 0.65$:

$$\left[\overline{\varphi}(0), \overline{u}_L(0)\right]\Big|_{\hat{\overline{U}}=0.7} \in \left[\overline{\varphi}(t), \overline{u}_L(t)\right]\Big|_{\hat{\overline{U}}=0.65} \qquad (7a)$$

Which pair of values $\left[\overline{\varphi}(t), \overline{u}_L(t)\right]\Big|_{\hat{\overline{U}}=0.65}$ will be the pair of initial values $\left[\overline{\varphi}(0), \overline{u}_L(0)\right]\Big|_{\hat{\overline{U}}=0.7}$ depends on the moment of increasing of the voltage source amplitude.

Similar, in a case of decreasing of the voltage source amplitude $\hat{\overline{U}}$ the values of initial conditions, $\overline{u}_L(0)$ and $\overline{\varphi}(0)$, for the value of voltage source amplitude $\hat{\overline{U}} = 0.7$ can be equal to any pair of instantaneous values, $\overline{u}_L(t)$ and $\overline{\varphi}(t)$, that are obtained at the value of voltage source amplitude $\hat{\overline{U}} + \Delta\hat{\overline{U}} = 0.75$:

$$\left[\overline{\varphi}(0), \overline{u}_L(0)\right]\Big|_{\hat{\overline{U}}=0.7} \in \left[\overline{\varphi}(t), \overline{u}_L(t)\right]\Big|_{\hat{\overline{U}}=0.75} \qquad (7b)$$

Figs. 7 show blue trajectories of coil flux and voltage $\overline{\varphi}(t)$ and $\overline{u}_L(t)$ at the value of the voltage source amplitude $\hat{\overline{U}} = 0.65$. According to (7a), in a case of increasing of the voltage source amplitude these values are the possible values of initial conditions, $\overline{u}_L(0)$ and $\overline{\varphi}(0)$, for the voltage source amplitude $\hat{\overline{U}} = 0.7$.

Thereby, the blue square marks the pair of initial condition values that are noted by increasing of the voltage source amplitude during the preliminary simulations described in section 4.

The ferroresonant jump can not occur for any combination of initial conditions if the trajectory of the coil voltage and flux (blue line on Fig. 7) passes through black area only. Consequently, if the trajectory passes through white area only, the ferroresonant will occur for every combination of initial conditions.

However, the results of simulations are based on a mathematical model. Thus, the limitation, as well as the applicability of the simulation results on physical models in general, depends on the accuracy of parameters of the mathematical model. For instance, the values of following parameters have a high impact on the initiation of steady-state types, but they are hard to obtain with a high accuracy:

a) Source voltage distortion, $u(t) \approx \hat{U} \sin \omega t$, caused by higher harmonics in power distribution network.

b) The change of bifurcation parameter (voltage source amplitude $\hat{\bar{U}}$) is not instantaneous. It depends on chosen laboratory equipment (variable autotransformer in particular case).

c) The magnetization characteristic of nonlinear iron-core coil (3).

d) The nonlinear characteristic of the iron-core losses (in the particular case approximated by linear resistor $\bar{R}$).

Therefore, by analysing the ferroresonant system, the whole 2-parameter bifurcation diagram should be considered as an illustration, which implies the odds of the initiation of a particular steady-state type or ferroresonance in general.

Fig. 9 shows 2-parameter bifurcation diagrams obtained for following values of voltage source amplitude:

$$\hat{\bar{U}} = 0.8, 0.9, 1.0$$

Values of initial conditions of voltage $\bar{u}_L$ and flux linkage $\bar{\varphi}$ where varied as in the preliminary simulations (4, 5). All other parameters were fixed.

Regarding the rotational symmetry, there is no need to obtain 2-parameter bifurcation diagrams for phase shift values $\alpha \geq \pi$. Thus, the following 2-parameter bifurcation diagrams shown on Fig. 9 were obtained for following phase shift values only:

$$\alpha = k\frac{\pi}{4}; \quad k = 0, 1, 2, 3 \qquad (8)$$

For four different phase shift values (8), values of voltage source amplitude $\hat{\bar{U}} = 1.1, 1.2, ..., 1.7$ and initial values defined by (4) and (5), all obtained steady-states were the odd higher harmonic steady-states.

At the same way as on the Fig. 7, the Fig. 9 shows the blue trajectory of coil flux and voltage, $\bar{\varphi}(t)$ and $\bar{u}_L(t)$, at the previous value of the voltage source amplitude in a case of increasing of the amplitude, i.e. at the value $\hat{\bar{U}} - \Delta\hat{\bar{U}}$. The blue squares mark the pairs of initial condition values that are noted by increasing of the voltage source amplitude during the preliminary simulations described in section 4.

■ Monoharmonic steady-state
□ Odd higher harmonic steady-state

a) $\hat{\bar{U}} = 0.8$

b) $\hat{\bar{U}} = 0.9$

c) $\hat{\bar{U}} = 1.0$
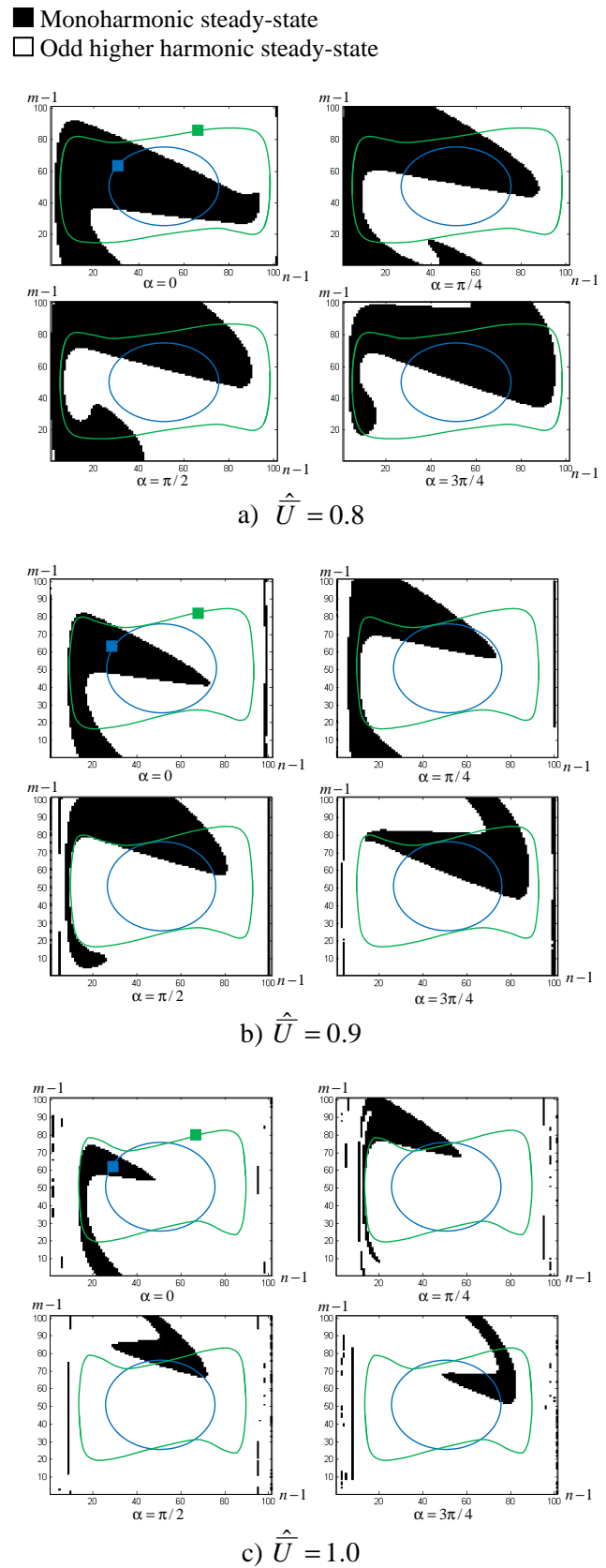
Fig. 9. The 2-parameter bifurcation diagrams for voltage source amplitude values $\hat{\bar{U}} = 0.8, 0.9, 1.0$

On Figs. 9 the green trajectory is the trajectory of coil flux and voltage, $\overline{\varphi}(t)$ and $\overline{u}_L(t)$, at the previous value of the voltage source amplitude in a case of decreasing of the amplitude, i.e. at the value $\hat{\overline{U}} + \Delta\hat{\overline{U}}$. The green squares mark the pairs of initial condition values that are noted by decreasing of the voltage source amplitude during the simulations described in section 4.

Figs. 7 and 9 reveal the impact of initial conditions on the initiation of odd harmonic steady-state ($\square$) and monoharmonic steady-state ($\blacksquare$) for voltage source amplitude values $0.7 \leq \hat{\overline{U}} \leq 1.0$. Depending on the values of phase shift α and initial conditions $\overline{u}_L(0)$ and $\overline{\varphi}(0)$, for voltage source amplitude values $0.7 \leq \hat{\overline{U}} \leq 1.0$, the initiation of monoharmonic steady-state is possible (part of trajectories on black area) as well as initiation of odd higher harmonic steady-state (part of trajectories on white area). It can be noticed that by increasing of the voltage source amplitude the white area is increasing, i.e. the range of pairs of initial condition values at which the initiation of odd higher harmonic steady-state is possible.

Hence, the initial conditions have a significant impact on the initiation of ferroresonant jump and reverse ferroresonant jump.

5.2 Odd higher harmonic steady-state and even and odd higher harmonic steady-state

The pitchfork bifurcation, i.e. the change from odd higher harmonic steady-state to even and odd higher harmonic steady-state, was not obtained by preliminary, as well as by additional simulations for values of voltage source amplitude $0 < \hat{\overline{U}} \leq 1.7$.

In this section are presented results of simulations that are carried out for voltage source amplitude values $1.7 < \hat{\overline{U}} < 2.35$. Thereby, the value of phase shift was set to $\alpha = 0$; and initial values were varied as follows:

$$\overline{u}_L(0)_m = \hat{\overline{U}}\left(\frac{m}{50} - 1\right); \quad m = 0,1,...,100 \qquad (9)$$

$$\overline{\varphi}(0)_n = \frac{\hat{\overline{U}}}{\overline{\omega}}\left(\frac{n}{50} - 1\right); \quad n = 0,1,...,100 \qquad (10)$$

For values of voltage source amplitude $1.7 < \hat{\overline{U}} \leq 1.75$ obtained steady-state types are odd higher harmonic steady-states for all initial conditions values defined by (9) and (10).

For values of voltage source amplitude $\hat{\overline{U}} = 1.76, 1.77$ there is a noticed impact of initial conditions on the initiation of odd higher harmonic steady-state ($\square$) and even and odd higher harmonic steady-state ($\blacksquare$), i.e. on the pitchfork bifurcation, Fig. 10.

$\square$ Odd higher harmonic steady-state
$\blacksquare$ Even and odd higher harmonic steady-state

a) $\hat{\overline{U}} = 1.76$

b) $\hat{\overline{U}} = 1.77$
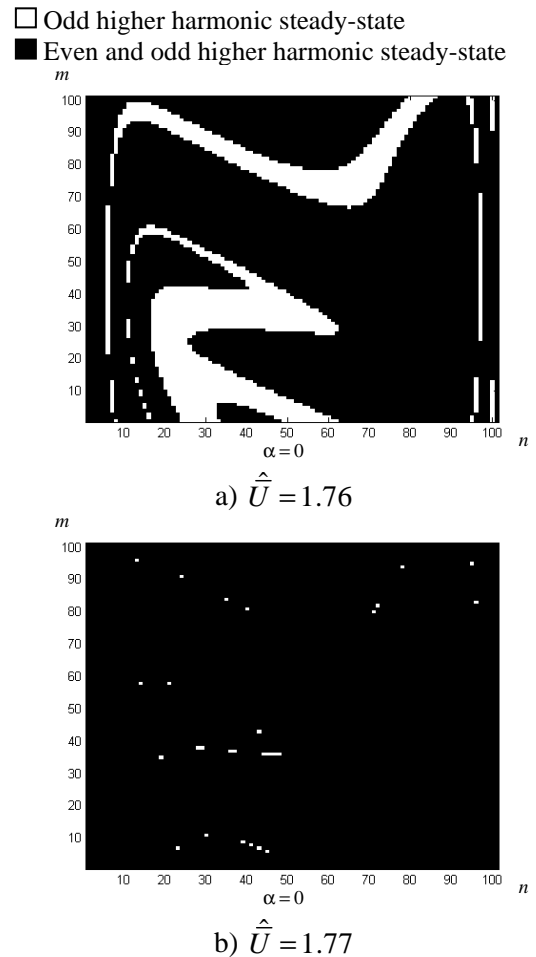
Fig. 10. The 2-parameter bifurcation diagrams for voltage source amplitude values $\hat{\overline{U}} = 1.76, 1.77$.

Steady-states obtained for values of voltage source amplitude $1.78 \leq \hat{\overline{U}} < 2.35$, were even and odd higher harmonic steady-states for all values of initial conditions defined by (9) and (10).

In laboratory measurements, the pitchfork bifurcation occurs at $\hat{\overline{U}} = 1.4$. As already mentioned, the pitchfork bifurcation was not obtained by preliminary, as well as by additional simulations for values of voltage source amplitude $0 < \hat{\overline{U}} \leq 1.7$. The disagreement between the measurements and simulation results could be lessen by improving the mathematical model of

ferroresonant circuit (more accurate nonlinear magnetization characteristic with nonlinear iron-core losses included; impedance of voltage source, winding resistance and capacitance of the coil added to the model of ferroresonant circuit) and by a simulation carried out with source voltage distorted according to real electrical power network voltage waveform. However, the further analysis of this problem is not the subject of this article.

5.3 Subharmonic and chaotic steady-state

In this section are presented results of simulations that are carried out for values of voltage source amplitude $2.35 \leq \hat{\bar{U}} \leq 3$, Fig. 11. Thereby, the value of phase shift was set to $\alpha = 0$, and initial values were varied as defined by (9) and (10).

■	Chaotic steady-state
■	Even and odd higher harmonic steady-state
■	Odd higher harmonic steady-state
■	Monoharmonic steady-state
■	Subharmonic steady-state (period-2)
■	Subharmonic steady-state (period-3)
■	Subharmonic steady-state (period-4)
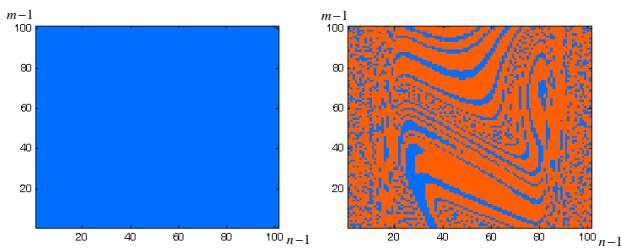
a) $\bar{\hat{U}} = 2.35$ b) $\bar{\hat{U}} = 2.4$
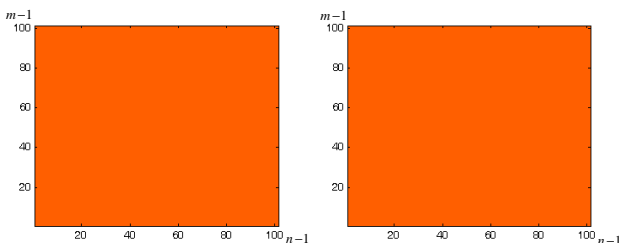
c) $\bar{\hat{U}} = 2.45$ d) $\bar{\hat{U}} = 2.5$
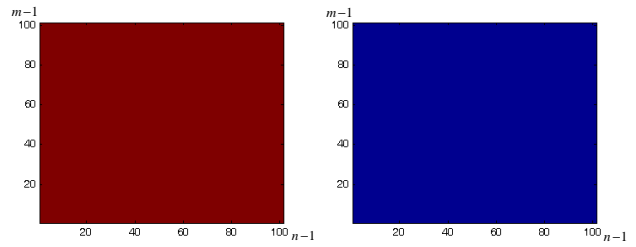
e) $\bar{\hat{U}} = 2.55$ f) $\bar{\hat{U}} = 2.6$
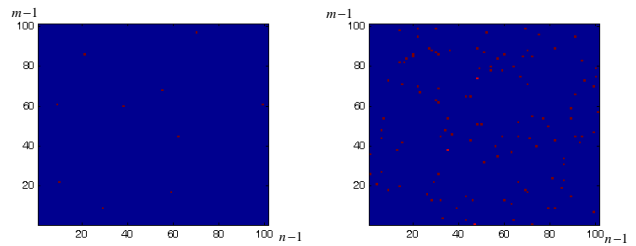
g) $\bar{\hat{U}} = 2.65$ h) $\bar{\hat{U}} = 2.7$
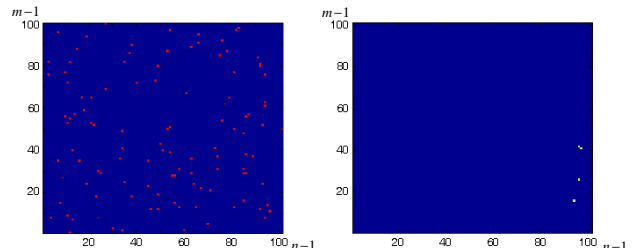
i) $\bar{\hat{U}} = 2.75$ j) $\bar{\hat{U}} = 2.8$
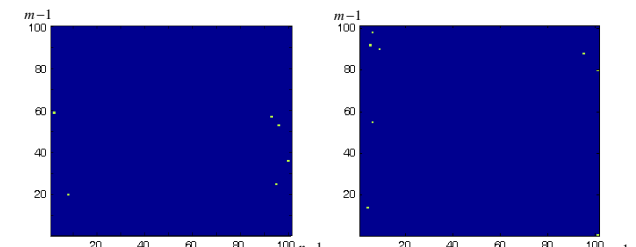
k) $\bar{\hat{U}} = 2.85$ l) $\bar{\hat{U}} = 2.9$
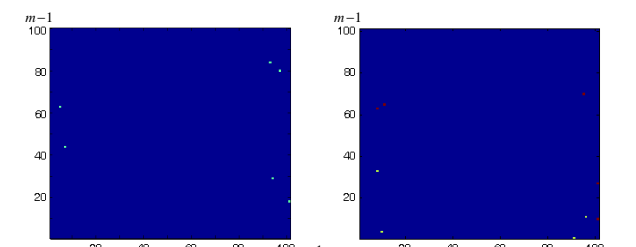
m) $\bar{\hat{U}} = 2.95$ n) $\bar{\hat{U}} = 3$

Fig. 11. The 2-parameter bifurcation diagrams for voltage source amplitude values $\bar{\hat{U}} = 2.35, 2.4, ..., 2.95, 3$ $(\alpha = 0)$.

For chosen values of the voltage source amplitude, there is an impact of initial conditions on the initiation of period-2 steady-state, Fig.11b. For values of voltage source amplitude $2.35 \leq \hat{\bar{U}} \leq 3$ prevails chaotic steady-state. However, for some pairs of initial conditions occur the periodic steady-states also.

6 Conclusions

By fixing the value of voltage source amplitude and varying the initial condition values of transformer voltage and flux linkage for eight different values of phase shift of voltage source ($\alpha_k = k \cdot \pi/4$; $k=0, \ldots, 7$), the initial conditions have been shown to have a clear definite impact on the initiation of fundamental frequency ferroresonance.

The steady-states obtained for values $\alpha_k = k \cdot \pi/4$, ($k = 0, 1, 2, 3$) are symmetric to the steady-states obtained for values $\alpha_k = k \cdot \pi/4$, ($k = 4, 5, 6, 7$) respectively, with respect to the angle π. Therefore, to investigate the impact of initial conditions on the initiation of fundamental frequency ferroresonance, it is necessary to carry out the simulations for values of voltage source phase $0 \leq \alpha < \pi$ only.

In a physical model the combinations of values of initial conditions are limited. Namely, the values of initial conditions are determined by the previous state of the system. Therefore, the steady-state types can be determined using the 2-parameter bifurcation diagrams and trajectory of coil flux and voltage $\overline{\varphi}(t)$ and $\overline{u}_L(t)$ that are obtained at the previous state of the system, i.e. at the previous value of the voltage source amplitude.

However, the validity of the 2-parameter bifurcation diagrams obtained by simulation depends on the accuracy of parameters of the mathematical model. Therefore, the steady-state of the ferroresonant circuit can not be predicted exactly, but the odds for the initiation of certain steady-state type can be estimated from a 2-parameter bifurcation diagram for a chosen range of initial condition values.

The ferroresonance in the electrical power system is an undesirable phenomenon often with harmful consequence. During the electrical power system design process, all possible initial conditions must be considered to identify potentially unstable states and to avoid the ferroresonance.

The 2-parameter bifurcation diagram is a practical and powerful presentation of the ferroresonant system and its possible steady-state types. However, predicting of the steady-state types of the ferroresonant or similar nonlinear systems is a difficult and time-consuming process because of:
a) determination of a mathematical model and its parameter values
b) long-standing numerical calculations for the creation of 2-parameter bifurcation diagrams

Further research will address the impact of losses on the appearance of 2-parameter bifurcation diagrams of the ferroresonant circuit.

References:
[1] IEEE Working Group, "Modelling and analysis guidelines for slow transients – part III: The study of ferroresonance," *IEEE Transactions on Power Delivery*, Vol. 15, No. 1, pp. 255-265, 2001.
[2] C. Kieny, "Application of the bifurcation theory in studying and understanding the global behavior of a ferroresonant electric power circuit," *IEEE Trans. Power Delivery*, Vol. 6, pp. 866–872, 1991.
[3] S. Mozaffari, S. Henschel, and A. C. Soudack, "Chaotic ferroresonance in power transformers," *Proc. IEE Generation, Transmission Distrib.*, Vol. 142, No. 3, pp. 247–250, 1995.
[4] J.R.Marti, A.C.Soudack, "Ferroresonance in power systems: Fundamental solutions," *IEE Proceedings-C*, Vol. 138, No. 4, pp. 321-329, 1991.
[5] V. Avrutin, M. Schanz, "On special types of two- and three-parametric bifurcations in piecewise-smooth dynamical systems", *WSEAS Transactions on Mathematics*, Issue 3, Volume 4, July 2005.
[6] F. B. Amar, R. Dhifaoui, "Bifurcation Diagrams and Lines of Period-1 Ferroresonance", *WSEAS Transactions on Power Systems*, Issue 7, Volume 1, July 2006
[7] B.Lee, V.Ajjarapu, "Period-doubling route to chaos in an electrical power system," *IEE Proceedings-C*, Vol. 140, No. 6, pp. 490-496, 1993.
[8] A.E.A. Araujo, A.C.Soudack, J.R.Marti, "Ferroresonance in power systems: Chaotic behaviour," *IEE Proceedings-C*, Vol. 140, No. 3, pp. 237-240, 1993.
[9] Z. Emin, B. A. T. Al Zahawi, D. W. Auckland and Y.K. Tong, "Ferroresonance in Electromagnetic Voltage Transformers: A Study Based on Nonlinear Dynamics," *IEE Proc.-Generation, Transmission, Distribution*, Vol. 144, No. 4, July 1997, pp. 383-387.

[10] Sinuhé Benítez, Leonardo Acho, and Julio C. Rolón G., "Chaos Generator via SCR Relaxation Oscillator", *WSEAS Transactions on Circuits and Systems*, Issue 2, Volume 3, April 2004.

[11] D. Negoitescu, D. Lascu, V. Popescu, C. Ivan, "Chaotic Behavior of the Buck-Boost Converter under Current-Mode Control " *12th WSEAS International Conference on Circuits*, Heraklion, Greece, July 22-24, 2008, pp. 125-130.

[12] I. N. Stouboulos, I. M. Kyprianidis, and M. S. Papadopoulou, "Initial Conditions and Coexisting Attractors in an Autonomous Circuit", *Proc. of the 5th WSEAS Int. Conf. on Non-Linear Analysis, Non-Linear Systems and Chaos*, Bucharest, Romania, October 16-18, 2006, pp. 87-91.

[13] R.W. Clark, G.C. Philippatos, "Chaos and Complexity in Finance and Economics", *WSEAS Transactions on Business and Economics*, Issue 1, Volume 1, January 2004.

[14] K. Miličević, D. Pelin, I. Flegar, "Measurement system for model verification of nonautonomous second-order nonlinear systems", *Chaos, Solitons & Fractals*, vol. 38, no.4, pp. 939-948, November 2008.

[15] I.Flegar, D.Fischer, D.Pelin "Identification of chaos in a ferroresonant circuit," *IEE Power Tech '99 Conference*, Budapest, Hungary, August 29-September 2, 1999; pp. 1-5, 1999.

[16] The MathWorks – MATLAB and Simulink for Technical Computing. 4th of January 2008. http://www.mathworks.com/access/helpdesk/help/toolbox/simulink/index.html?/access/helpdesk/help/toolbox/simulink/ug/f11-69449.html